Quantification of the forces driving self-assembly of three-dimensional microtissues

Jacquelyn Youssef[a,b], Asha K. Nurse[c], L. B. Freund[b,c,1], and Jeffrey R. Morgan[a,b,1]

[a]Department of Molecular Pharmacology, Physiology and Biotechnology, [b]Center for Biomedical Engineering, and [c]School of Engineering, Brown University, Providence, RI 02912

In a nonadhesive environment, cells will self-assemble into microtissues, a process relevant to tissue engineering. Although this has been recognized for some time, there is no basis for quantitative characterization of this complex process. Here we describe a recently developed assay designed to quantify aspects of the process and discuss its application in comparing behaviors between cell types. Cells were seeded in nonadhesive micromolded wells, each well with a circular trough at its base formed by the cylindrical sidewalls and by a central peg in the form of a right circular cone. Cells settled into the trough and coalesced into a toroid, which was then driven up the conical peg by the forces of self-assembly. The mass of the toroid and its rate of upward movement were used to calculate the cell power expended in the process against gravity. The power of the toroid was found to be 0.31 ± 0.01 pJ/h and 4.3 ± 1.7 pJ/h for hepatocyte cells and fibroblasts, respectively. Blocking Rho kinase by means of Y-27632 resulted in a 50% and greater reduction in power expended by each type of toroid, indicating that cytoskeletal-mediated contraction plays a significant role in the self-assembly of both cell types. Whereas the driving force for self-assembly has often been viewed as the binding of surface proteins, these data show that cellular contraction is important for cell–cell adhesion. The power measurement quantifies the contribution of cell contraction, and will be useful for understanding the concerted action of the mechanisms that drive self-assembly.

3D cell culture | cellular mechanics | systems biology | multicellular aggregate

The self-assembly of cells into microtissues, often viewed as a passive process driven by chemical forces resulting from binding of cadherins expressed on cell surfaces (1, 2), is now thought to be a more complex process. Recent work has shown that the cytoskeleton also plays an important role in force generation, stability, and self-sorting of microtissues (3–6). Thus, self-assembly is a complex process involving multiple protein mechanisms working in concert.

Self-assembly and the cell–cell adhesion that drives it are relevant to tissue formation, morphogenesis, and disease. However, little quantitative data are available on the forces driving self-assembly. At the molecular level, precise measurements of the binding strength and energy of adhesion of surface proteins (7, 8) as well as the force of contraction of the actin cytoskeleton (9, 10) have been made. On the cellular level, traction-force microscopy has been used to measure the adhesion forces of single cells on flat substrates (11–13), and fibroblast-populated collagen gels have been used in the study of cell–matrix interactions (14). However, cell–cell interactions in a 3D environment have not been fully investigated. Doing so requires a quantitative systems biology approach that can be used not only to quantify the aggregation and self-assembly of groups of cells but also to quantify the contributions of specific proteins and protein systems to the process.

In the past, we have reported observations on the behavior of monodispersed normal human fibroblasts (NHFs) when seeded in a nonadhesive micromolded hydrogel cylindrical well (15). For the case of a well with a base in the form of a circular trough defined by the outer surface and a central conical peg, the cells rapidly self-assembled into a microtissue in the form of a multicellular toroid. The forces of self-assembly were strong enough to drive the toroid up the slope of the peg from its base to its summit (4). Here we describe a unique assay to measure these forces. In particular, the assay provides a measure of cell power defined as the rate of work done against gravity as such a self-assembled multicellular toroid moves up a conical peg of known geometry. The assay was used to compare behaviors of two cell types, the NHF and a rat hepatocyte cell line (H35). We found that, regardless of the slope of the conical peg, rapidly self-assembling NHF toroidal microtissues reached a particular height in just 2 h, whereas the H35 toroids assembled more slowly and required at least 48 h to reach the same prescribed height for all slopes considered. These data were used to calculate the power of NHF toroids, which was found to be an order of magnitude greater than that of the H35 toroids.

In addition to these comparisons, the contributions to the cell power of specific protein systems were quantified. When treated with the Rho kinase (ROCK) inhibitor Y-27632, power output of an NHF toroid decreased by ∼50%. When H35 toroids were treated with the same inhibitor, their power output decreased by 85%, an unexpected result, as H35s are not considered to be a contractile cell type. These data indicate that active cellular contraction has an important role in the self-assembly of both highly contractile NHFs as well as the noncontractile H35s. The assay has the advantage of being a straightforward noninvasive, noncontact method for measuring the forces of self-assembly. Cell power is a quantitative systems biology measurement for comparing the behavior of different cell types with the potential to quantify the contributions of specific proteins or protein systems to the complex process of self-assembly.

Results

To investigate the forces governing the self-assembly of 3D microtissues from monodispersed cells, we chose the toroid and designed a 3D micromold made of polyacrylamide (Fig. 1). This nonadhesive micromold contained a single row of toroid wells. To vary loading conditions, we fabricated micromolds with conical pegs of differing slopes which were measured to be 84.2 ± 2.6° (85°), 65.9 ± 4.9° (65°), and 55.1 ± 3.4° (55°). When a cell suspension was seeded, the cells settled to the bottom of the circular trough and were confined by the chamber wall at the outer edge of the trough and by a conical peg on the inner edge of the trough. As a result of cell–cell interactions, they assembled into toroidal microtissues. The integrity and symmetry of the

CELL BIOLOGY

www.manaraa.com
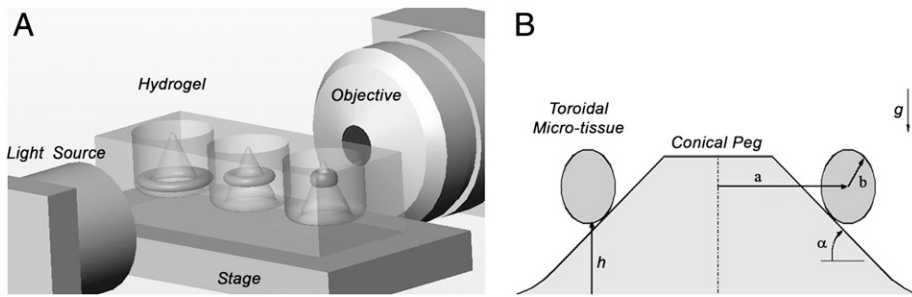
Fig. 1. Schematic of experimental system to quantify the forces of self-assembly. (*A*) Monodispersed cells aggregate and form toroidal microtissues. The forces of self-assembly drive the toroid up the slope of the conical peg, and this movement can be captured by side-view microscopy. (*B*) Schematic of a cross-section of a toroidal microtissue on a conical peg. Denoted are the height moved by the microtissue (*h*), the slope of the conical peg (α), the direction of gravity (*g*), and the major and minor radii (a) and (b).

toroid were maintained, with the forces of self-assembly tending to drive the toroid up the cone (Fig. 2) (Movies S1 and S2).

To determine the minimum number of cells needed to form a toroid, we seeded micromolds with varying numbers of either NHFs or H35s and assessed toroid formation after 17 h for three slopes (Fig. 3). For both cell types, toroid formation was 100% for all three slopes when seeded with 21,000 cells per toroid or greater. The cell number at which toroid formation was 50% for NHFs was 8,000, 6,000, and 5,000 cells for the 85°, 65°, and 55° slopes, respectively, and for the H35s it was 3,000 cells for all three slopes. These data suggest that the initial and rapid events of NHF toroid formation are slope (load)-sensitive but, once formed, the NHF toroid is stable and progresses rapidly. For subsequent experiments, we seeded micromolds with 21,000 cells per well for both cell types to assure 100% toroid formation and to minimize size.

Using side-view microscopy, we measured the vertical distance traveled by the toroid (height), its major radius, and its minor radius as it moved up the three slopes. Over an 8-h period, the height of NHF toroids increased with time and was comparable for all three slopes (Fig. 4). In contrast, H35 toroids climbed the conical pegs at a much slower rate. Within 2 h, NHF toroids moved an average of almost 170 μm for all three slopes, whereas H35 toroids were much slower and required 48, 72, and 96 h on the 55°, 65°, and 85° slopes, respectively, to reach the height NHF toroids had attained in only 2 h. Unlike the NHFs, the distance traveled by the H35 toroids was dependent on the slope of the peg, with samples on the 65° and 85° slopes climbing an average of 33 and 50 μm less, respectively, in the first 24 h, than the 55° samples. By changing the slope of the peg from 55° to 65°, the component of the toroid's weight opposing its motion is increased by 10%. Likewise, the change from 55° to 85° results in an 18% increase in loading. For H35 toroids, a 10% increase in loading (55° to 65°) decreased the height 28%, whereas an 18% increase in loading (55° to 85°) led to a 42% decrease in toroid height.

The values for the major and minor radii were used to calculate the volume of each toroid for the duration of the experiments using the equation $V = 2\pi^2 ab^2$, where *a* is the major radius and *b* is the minor radius. Changes to the volume of the toroid for all three slopes were not statistically significant, with volume fluctuations being less than 4.4%, 1.6%, and 1.6% for the 85°, 65°, and 55° slopes, respectively, for the NHF microtissues and less than 0.5%, 3.6%, and 4.7% for the 85°, 65°, and 55° slopes, respectively, for the H35 microtissues.

The cellular forces of self-assembly that drive the toroid up the cone must overcome the gravitational forces resisting its movement. To estimate the mass of the toroid, we measured the density of individual cells in cell-culture medium and computed density from the settling rate. The density of single NHF and H35 cells was 1.05 ± 0.01 and 1.08 ± 0.02 g/cm^3, respectively. Thus, based on toroid volume and density of the cells, we calculated that a toroid of 21,000 NHFs has a mass of 4.36 μg and a toroid of the same number of H35s has a mass of 6.98 μg.

The rate at which the cellular forces of self-assembly work to move a toroid up the cone is power: $P = \Delta W / \Delta t$, where ΔW is work necessary to move a toroid of a given mass to a given height and Δt is the time over which the work is performed. Cell power is an indication of the rate of self-assembly in terms of the energy output. From measurements of toroid height and weight, we calculated cell power as a function of time (Fig. 4). For both cell types, cell power gradually decreased over the course of the experiments; however, only the cell power of H35 toroids was dependent on slope. Specifically, at 2 h, the power output of an NHF toroid was 3.8 ± 0.9, 4.1 ± 1.6, and 4.7 ± 1.6 pJ/h for the 85°, 65°, and 55° slopes, respectively, whereas the power exerted by an H35 toroid of the same cell number to a height comparable to that of an NHF toroid was only 0.24 ± 0.01, 0.31 ± 0.01, and 0.49 ± 0.04 pJ/h for the 85°, 65°, and 55° slopes, respectively. If we assume that all cells within a microtissue exert equal power, the power per cell for all three slopes averaged to 0.2 fJ/h per NHF and 0.02 fJ/h per H35. For an H35 toroid to reach the height of an NHF toroid in the same time, it would have to increase its power output by about 93%.

To elucidate the contribution of cytoskeletal-mediated contraction in terms of cell power, NHFs and H35s were treated
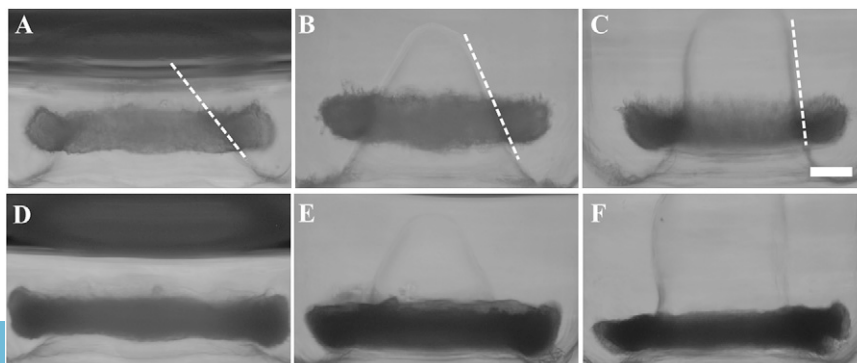
Fig. 2. Self-assembling NHF and H35 toroids travel up conical pegs at different rates. NHFs (*A*–*C*) and H35s (*D*–*F*) were seeded in micromolded polyacrylamide gels with toroidal recesses and side-view images were obtained. Central conical pegs were designed with 55° (*A* and *D*), 65° (*B* and *E*), and 85° (*C* and *F*) slopes (dotted lines are added to accentuate slope). H35 microtissues reach the height that NHF microtissues reach in 2 h (*A*–*C*) in 48 h (*D*–*F*). (Scale bar, 200 μm.)

Youssef et al.

www.manaraa.com
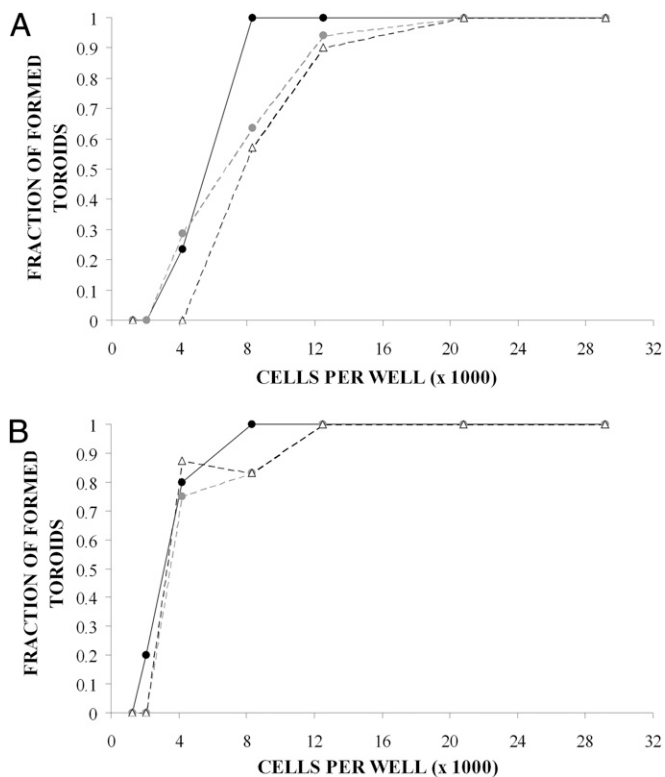
Fig. 3. Toroid formation was cell number-dependent. Different numbers of NHFs (*A*) and H35s (*B*) were seeded in toroidal wells with 55° (black circles), 65° (gray circles), and 85° (triangles) slopes. The percentage of intact toroids was determined 17 h after cell seeding. Sample size (n) is greater than 5 for all points.

with 10 and 100 μM Y-27632, an inhibitor which blocks ROCK-mediated contraction by preventing the formation of stress fibers and the phosphorylation of myosin light chains. Treated cells were seeded in micromolds equilibrated in Y-27632, and side-view images were taken at 2-h intervals for 8 h for NHFs and at 24-h intervals for 96 h for H35s. Y-27632-treated toroids still moved up the conical pegs, but did not climb as high as the untreated controls for both NHFs and H35s (Fig. 5). Specifically, significant differences were seen between controls and treated samples (10 and 100 μM Y-27632) for all three slopes. Toroid height and weight were used to analyze the power output of the NHFs (Table 1). After 2 h, inhibiting ROCK (with both 10 and 100 μM Y-27632) led to a $49 \pm 9\%$ decrease in power for NHFs. Similar to NHFs, H35-treated toroids did not climb as high as control samples, with ROCK inhibition decreasing H35 toroid height for all three slopes in a dose-dependent manner. Toroid

sensitivity to slope was also exhibited, with 65° and 85° drug-treated samples stalling completely at later time points whereas the 55° drug-treated samples continued up the cone for the duration of the experiment. ROCK inhibition also substantially decreased H35 power output, with an average power decrease of $58 \pm 7\%$ for the 10 μM and $83 \pm 2\%$ for the 100 μM Y-27632-treated samples over all time points.

Discussion

Most studies on the cell–cell adhesion that drives self-assembly are qualitative and have focused on the self-sorting of a mixture of cells (1, 16), the role of cadherins (17), and the influence of surface tension (1, 2). In this study, we have developed a unique assay to measure cell power, a quantitative measure of the work output of self-assembling cells. The assay is well-suited to measuring the small forces of self-assembly that occur with relatively slow kinetics in groups of living cells. Unlike other assays, which use compression testing (16), the assay does not contact or manipulate the microtissues, which could alter its properties. Because the assay incorporates only time and the influence of gravity, loads on the microtissues are precise and reproducible and instrument calibrations are unnecessary. The geometry of the cone can be carefully controlled, reproduced, and measured. Moreover, the influence of gravity can be modulated by changing the slope of the cone to induce a variety of loading conditions.

A power measurement is a systems quantitative measure of a multicomponent system (mechanical, chemical, and surface energy) that drives self-assembly. Much attention has been focused on the role of cadherins, and it has been shown that within a single cell type, expression of cadherins has a strong influence on self-assembly (2). However, it has also been shown that cytoskeletal-mediated tension affects self-assembly (3, 6). Further, it is well-known that in addition to cadherins, cells have numerous other surface proteins responsible for cell–cell adhesion and that the types of these proteins and their levels vary widely between different cell types, as do the proteins that participate in cytoskeletal-mediated tension (18–22). A power measurement takes into account the action of all these protein systems as well as those that might act to resist cell–cell adhesion such as differences in the stiffness and viscoelasticity of cells or levels of antiadhesive proteins. Power measurements can be used as a point of reference for comparing cell types. We have observed that the driving forces behind the self-assembly of NHFs are significantly greater than those of H35s and are of a magnitude (strength and/or rate) that is unaffected (or unobservable) even under an 18% increase in loading.

Power measurements can also be used to quantify the specific contribution of cellular components to self-assembly. Recent work from our laboratory demonstrated that myosin motors participate in the stability (3, 5) and sorting (3) of NHF micro-

Table 1. NHF and H35 toroid power as a function of slope and Y-27632 concentration at 2 h for NHFs and averaged over all time points for H35s

|	NHF					
	85°		65°		55°	
Concentration Y-27632 (μM)	10	100	10	100	10	100
Power attributed to ROCK (pJ/h)	1.6	2.1	2.5	1.8	1.8	3.0
Decrease in power (%)	42	53	57	41	36	60
	H35					
	85°		65°		55°	
Concentration Y-27632 (μM)	10	100	10	100	10	100
Power attributed to ROCK (pJ/h)	0.09 ± 0.02	0.14 ± 0.03	0.15 ± 0.03	0.19 ± 0.03	0.20 ± 0.11	0.27 ± 0.11
Decrease in power (%)	51 ± 2	80 ± 3	65 ± 4	83 ± 5	59 ± 10	85 ± 2

Youssef et al.

www.manaraa.com
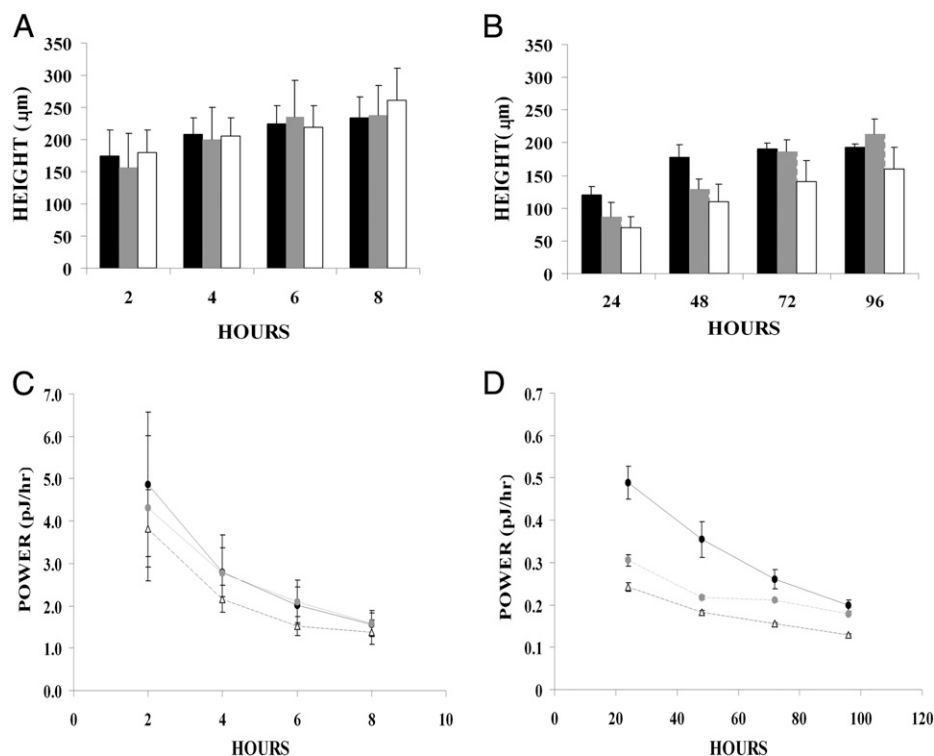
Fig. 4. NHF toroid height and power output were independent of slope and of a much greater magnitude than that of the H35s. The distance traveled by the toroids up the conical pegs was measured as a function of time and peg slope of 85° (white), 65° (gray), and 55° (black) for NHFs (*A*) and H35s (*B*). Movement of NHF toroids was rapid, and differences between slopes were not statistically significant. Movement of H35 toroids was slower, and the differences between the 85° and 65° slopes and the 85° and 55° slopes at 24 and 48 h were statistically significant. At 72 and 96 h, differences between the 85° and 55° and the 65° and 55° were statistically significant. Cell power was calculated as a function of potential energy over time for NHF (*C*) and H35 (*D*) microtissues for the 55° (black circles), 65° (gray circles), and 85° (triangles) slopes. The power output of H35 microtissues decreased substantially as the slope of the central peg increased ($P < 0.05$). For NHFs, $n = 7$, 9, and 6 for the 85°, 65°, and 55°, respectively. For H35s, $n = 9$, 8, and 5 for the 85°, 65°, and 55°, respectively. Error bars are SDs.

tissues, and others have shown their role in zebrafish embryos (6). When ROCK was inhibited in our experiments, power output of an NHF toroid decreased by about 50%. This result is not surprising for NHFs, a cell with well-known contractile properties; but, when ROCK was inhibited in H35 toroids, power output decreased by 85%, indicating the importance of the cytoskeleton in the self-assembly of both contractile and noncontractile cells. Although the power associated with ROCK in H35s is significantly lower than that of NHFs (0.25 compared with 2.1 pJ/h, respectively), ROCK-associated power is a larger proportion of the total power driving self-assembly of H35s compared with NHFs (85% versus 50%, respectively). Several reasons could

explain why ROCK contributes a larger percentage to H35 self-assembly. H35s are a denser cell (0.03 g/cm^3 greater than NHF) and so when cellular contraction is blocked, the effect of the cell's weight could be further amplified. When loading was decreased by lowering the slope of the peg, H35 toroids traveled farther up the peg, indicating that the weight of the microtissue is a limiting factor in its power output. Another possible explanation could be that NHFs have a radially arranged cytoskeletal network (3), whereas H35s, as an epithelial cell, have a cortically arranged cytoskeletal network (23). A radial cytoskeletal network may be more efficient at exerting power than a cortical cytoskeleton, and so an even higher dose of Y-27632 may be necessary to fully block
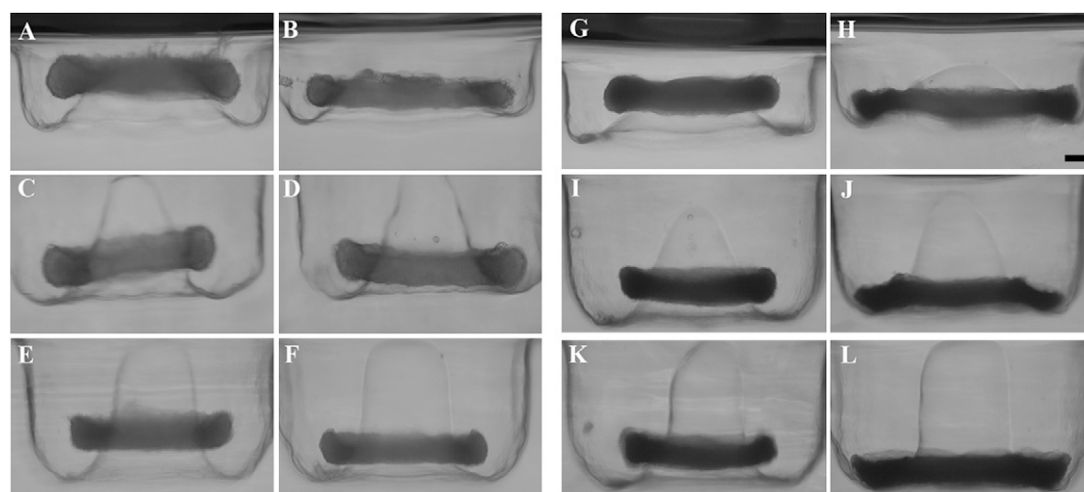
Fig. 5. Inhibition of ROCK-mediated contraction using Y-27632 impeded toroid motion up the conical peg of both NHFs and H35s. NHFs were treated with 0 (*A*, *C*, and *E*) and 100 (*B*, *D*, and *F*) μM Y-27632 and were seeded in drug-equilibrated gels with 55° (*A* and *B*), 65° (*C* and *D*), and 85° (*E* and *F*) slopes. As early as 2 h, drug-treated NHF samples were significantly lower on the peg than control samples. H35s were also treated with 0 (*G*, *I*, and *K*) and 100 (*H*, *J*, and *L*) μM Y-27632 and were seeded in drug-equilibrated gels with 55° (*G* and *H*), 65° (*I* and *J*), and 85° (*K* and *L*) slopes. The effect of drug treatment was visible after 24 h. (Scale bar, 200 μm.)

www.manaraa.com
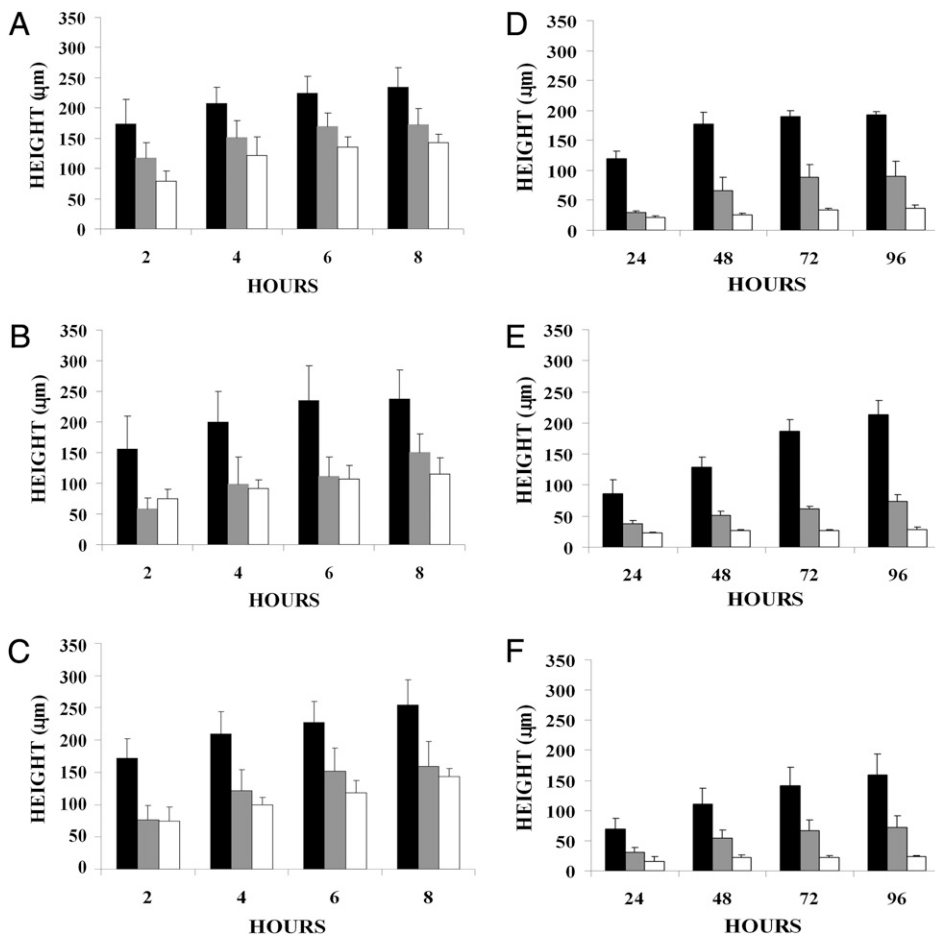
Fig. 6. Toroid height was dependent on Y-27632 concentration for both NHFs and H35s. For all slopes, ROCK inhibition decreased the final height reached of NHF microtissues ($P < 0.05$ between control and drug-treated samples). The motion of NHF-treated toroids was altered in a dose-dependent manner for the 55° slope (A) as the dose was increased from 0 (black) to 10 (gray) to 100 (white) μM. However, dose dependency was not observed for the 65° (B) and 85° (C) slopes, as 10 μM Y-27632 was sufficient to inhibit the motion of the microtissue to its fullest. ROCK inhibition altered the height achieved by H35 microtissues in a dose-dependent manner for all slopes (D–F are 55°, 65°, and 85°, respectively) ($P < 0.05$). Error bars represent SDs.

contraction in NHFs. A third reason may have to do with the pathways used for contraction. The ROCK system and the myosin regulatory light chain kinase system (MLCK) are two distinct pathways involved in contraction of NHFs (24, 25). By blocking the ROCK pathway in NHFs, the MLCK pathway may compensate and mask the full effect of blocking contraction. In addition, the MLCK pathway may not play as much of a role in the self-assembly of H35s as it does in NHFs. It is also possible that a greater proportion of NHFs' self-assembly power resides with its surface binding proteins due to higher expression and/or energy of these proteins.

One theory of self-assembly is that cells minimize surface free energy by maximizing intercellular adhesion (1). This theory also states that a mix of two different cell types will self-sort due to differences in adhesion and cohesion, like the behavior of two immiscible fluids (1). In this theory, the apparent surface tension is regarded as the sole factor determining the formation and structure of self-assembled microtissues. Within a single cell line it was demonstrated that spheroid surface tension was directly proportional to cadherin expression, with cells with increased cadherin levels moving to the center of mixed spheroids (2, 16, 17). With this model, the process of self-assembly was deemed to be passive and even likened to soap bubble formations (26). However, recent data have shown that the strength or specificity of cadherin bonds alone do not predict sorting behavior in self-assembly (7). Our power measurements reveal that self-assembly is not a passive process and that cytoskeletal-mediated tension is a major contributor for both cell types. In addition, because cell power takes a systems biology approach, it may be useful for predicting the sorting behavior of different cell types as well as the sorting behavior of one cell type when a population of the cells has been treated to decrease or increase the function of a specific protein.

Power measurements may be an interesting point of reference between measurements of the energies of purified proteins as well as protein systems from single cells. The power output by an NHF toroid is 2.5 pJ (between 2 and 4 h, 65° slope) and the energy of cadherin bonding is $4–48 \times 10^{-21}$ J per cadherin bond (27). This power output is equivalent to the formation of 52–625 million cadherin bonds. If cadherin bonding alone drove the 20,000-μm² change in toroid surface area that occurs over 2 h, we estimate it would require 2.6–31 thousand cadherins/μm² on the outer surface of the toroid (3–39 million cadherins per cell). When overexpressed by genetic modification there are 20,000–250,000 cadherins per cell, and in cadherin binding strength experiments (8) artificial monolayers have between 2,000 and 4,000 cadherins/μm² (27). Likewise, the force produced by focal adhesions of single cells is ~30 nN in a period of 5 min (10). A cell with ~25 focal adhesions would have a power output of ~4 fJ/h per cell, higher than our measure of 0.2 fJ/h per cell. However, it should be kept in mind that the focal adhesion measurements were made on a stiff substrate (megapascals) (10), and self-assembling microtissues are significantly less stiff (kilopascals) (11).

Last, unlike other models of self-assembly, a cell power analysis does not assume that the system is thermodynamically closed, nor is it confined by assumptions about how the system operates. For example, cell power does not assume that the system is driven solely by passive surface interactions (which ignores proteins inside the cell and the chemical energy derived

CELL BIOLOGY

from ATP), nor does cell power assume that the system is driven by the cytoskeleton alone, ignoring the binding of surface proteins. A cell power measurement quantifies the amount of energy expended and so is a useful point of comparison for cell types from different tissues. And, as our ROCK inhibition data show, it can be used to quantify the contribution of specific proteins and protein systems to self-assembly regardless of their cellular location or mechanism of action. Such information is important for a fundamental understanding of cell–cell adhesion and may be useful for applications in tissue engineering. For example, cell power measurements could be used with selected pharmacologies or genetic tools to tailor the tissue assembly process. Previously, we have shown that H35s will readily form a stable microtissue in the shape of honeycombs or a loop-ended dogbone; however, NHF microtissues in the same configuration will self-assemble, stretch, and ultimately fail (4, 5). NHF dogbone structures can be stabilized by treatment with Y-27632 (5). From this study, we know that drug-treated NHFs have a reduced power of 0.10 ± 0.01 fJ/h per NHF, and so power measurements may be useful for predicting the stability of complex shaped microtissues. Power measurements may also be useful for understanding the self-sorting of mixtures of cells with those cells of higher cell power occupying the core of a spheroid. In a prior study, NHFs treated with Y-27632 formed the outer coating when mixed with untreated NHFs, and in mixes of NHFs and H35s, NHFs formed the inner core (3).

Materials and Methods

Micromold Design and Gel Casting. Toroid molds were designed using the computer-aided design (CAD) software SolidWorks (SolidWorks). Three mold geometries were designed in which the slope of the central peg was modified to be 85°, 65°, and 55°. The circular round bottom troughs were 400, 350, and 300 μm in diameter and the central pegs were 600, 650, and 780 μm for the 85°, 65°, and 55° slopes, respectively. For the 85° and 65° slopes the micromolds contained 12 wells and for the 55° slope 11 wells. CAD files were used to produce thermowax molds with a rapid prototyping machine (3D Systems).

The wax molds were used to cast 13% polyacrylamide gels. Gels were removed from the wax molds and transferred to six-well culture plates. The gels were rinsed with fresh culture medium and then equilibrated overnight at 37 °C in 4 mL of DMEM supplemented with 10% FBS and 1% penicillin/streptomycin (pen/strep). After equilibration, the medium was removed and the gels were rinsed with fresh medium.

Cell Culture and Gel Seeding. NHFs (passages 3–10), derived from neonatal foreskins, and H35s (passages 4–12) were grown in T-175 flasks in DMEM with 10% FBS and 1% pen/strep at 37 °C and 10% CO_2. Cells were removed from flasks using a standard trypsin process. Briefly, cells were exposed to 0.05% trypsin for 10 min, quenched with serum-containing medium, spun down at 800 rpm for 6 min, resuspended in a known volume of medium, and counted. Seventy microliters of cell solution was added to each hydrogel. After 30 min, 3 mL of fresh medium was added to each of the wells. Images of the samples were taken every 2 h for 8 h for NHFs and every 24 h for 96 h for H35s. To determine the minimum number of cells necessary to form a stable toroid, 1,000–30,000 cells per well were seeded in the 85°, 65°, and 55° gels. Toroid formation was assessed using side-view microscopy 17 h after seeding.

For drug inhibition studies, Y-27632 (Sigma-Aldrich) was dissolved in culture medium and brought to a stock concentration of 200 μM. The stock solution was further diluted in culture medium to obtain solutions with concentrations of 10 and 100 μM. Before cell seeding, gels were equilibrated for at least 2 h in drug-containing medium and cells were resuspended in drug-containing medium. Cells were then seeded in the gels and imaged.

Cell-Density Measurements. Monodispersed cells were pipetted into the micromolds and side-view time-lapse images were taken to measure the rate at which individual cells settled. Settling rates were used to calculate the density of the H35s and NHFs using a force balance for the drag force on a sphere moving at a constant speed through a viscous fluid. In the present instance, this balance is written in the form $\rho_{cell} = \rho_{medium} + (6\pi\mu vr)/gV$, where ρ_{cell} is the density of a cell, ρ_{medium} is the density of the medium, μ is the dynamic viscosity of the medium, v is the rate at which the cell settles, r is the radius of the cell, and V is the volume of the cell.

Thus, based on the volume of the toroid and the density of individual cells, we calculated that a toroid of 21,000 NHFs has a mass of 4.36 μg and a toroid of the same number of H35s has a mass of 6.98 μg.

Microscopy. To capture side-view images, a Mitutoyo FS110 microscope was modified to lie on its back and a translational stage was added to hold samples. Samples were imaged in bright field through the eyepiece of the microscope. ImageJ software (National Institutes of Health) was used to measure the height of the toroid, the major radius and minor radius of the toroid, and the slope of the conical pegs.

1. Steinberg MS (1962) Mechanism of tissue reconstruction by dissociated cells. II. Time-course of events. *Science* 137:762–763.
2. Foty RA, Steinberg MS (2005) The differential adhesion hypothesis: A direct evaluation. *Dev Biol* 278:255–263.
3. Dean DM, Morgan JR (2008) Cytoskeletal-mediated tension modulates the directed self-assembly of microtissues. *Tissue Eng Part A* 14:1989–1997.
4. Dean DM, Napolitano AP, Youssef J, Morgan JR (2007) Rods, tori, and honeycombs: The directed self-assembly of microtissues with prescribed microscale geometries. *FASEB J* 21:4005–4012.
5. Dean DM, Rago AP, Morgan JR (2009) Fibroblast elongation and dendritic extensions in constrained versus unconstrained microtissues. *Cell Motil Cytoskeleton* 66:129–141.
6. Krieg M, et al. (2008) Tensile forces govern germ-layer organization in zebrafish. *Nat Cell Biol* 10:429–436.
7. Shi Q, Chien YH, Leckband D (2008) Biophysical properties of cadherin bonds do not predict cell sorting. *J Biol Chem* 283:28454–28463.
8. Sivasankar S, Gumbiner B, Leckband D (2001) Direct measurements of multiple adhesive alignments and unbinding trajectories between cadherin extracellular domains. *Biophys J* 80:1758–1768.
9. Lan G, Sun SX (2005) Dynamics of myosin-driven skeletal muscle contraction: I. Steady-state force generation. *Biophys J* 88:4107–4117.
10. Tan JL, et al. (2003) Cells lying on a bed of microneedles: An approach to isolate mechanical force. *Proc Natl Acad Sci USA* 100:1484–1489.
11. Discher DE, Janmey P, Wang YL (2005) Tissue cells feel and respond to the stiffness of their substrate. *Science* 310:1139–1143.
12. Harris AK, Wild P, Stopak D (1980) Silicone rubber substrata: A new wrinkle in the study of cell locomotion. *Science* 208:177–179.
13. Dembo M, Wang YL (1999) Stresses at the cell-to-substrate interface during locomotion of fibroblasts. *Biophys J* 76:2307–2316.
14. Barocas VH, Moon AG, Tranquillo RT (1995) The fibroblast-populated collagen microsphere assay of cell traction force—Part 2: Measurement of the cell traction parameter. *J Biomech Eng* 117:161–170.
15. Napolitano AP, Chai P, Dean DM, Morgan JR (2007) Dynamics of the self-assembly of complex cellular aggregates on micromolded nonadhesive hydrogels. *Tissue Eng* 13:2087–2094.
16. Foty RA, Pfleger CM, Forgacs G, Steinberg MS (1996) Surface tensions of embryonic tissues predict their mutual envelopment behavior. *Development* 122:1611–1620.
17. Foty RA, Steinberg MS (2004) Cadherin-mediated cell-cell adhesion and tissue segregation in relation to malignancy. *Int J Dev Biol* 48:397–409.
18. Pokutta S, Weis WI (2007) Structure and mechanism of cadherins and catenins in cell-cell contacts. *Annu Rev Cell Dev Biol* 23:237–261.
19. Hartsock A, Nelson WJ (2008) Adherens and tight junctions: Structure, function and connections to the actin cytoskeleton. *Biochim Biophys Acta* 1778:660–669.
20. Unwin PN (1987) Gap junction structure and the control of cell-to-cell communication. *Ciba Found Symp* 125:78–91.
21. Chrzanowska-Wodnicka M, Burridge K (1996) Rho-stimulated contractility drives the formation of stress fibers and focal adhesions. *J Cell Biol* 133:1403–1415.
22. Goeckeler ZM, Wysolmerski RB (1995) Myosin light chain kinase-regulated endothelial cell contraction: The relationship between isometric tension, actin polymerization, and myosin phosphorylation. *J Cell Biol* 130:613–627.
23. Omelchenko T, et al. (2001) Contact interactions between epitheliocytes and fibroblasts: Formation of heterotypic cadherin-containing adhesion sites is accompanied by local cytoskeletal reorganization. *Proc Natl Acad Sci USA* 98:8632–8637.
24. Katoh K, Kano Y, Amano M, Kaibuchi K, Fujiwara K (2001) Stress fiber organization regulated by MLCK and Rho-kinase in cultured human fibroblasts. *Am J Physiol Cell Physiol* 280:C1669–C1679.
25. Katoh K, et al. (2001) Rho-kinase—Mediated contraction of isolated stress fibers. *J Cell Biol* 153:569–584.
26. Hayashi T, Carthew RW (2004) Surface mechanics mediate pattern formation in the developing retina. *Nature* 431:647–652.
27. Sivasankar S, Brieher W, Lavrik N, Gumbiner B, Leckband D (1999) Direct molecular force measurements of multiple adhesive interactions between cadherin ectodomains. *Proc Natl Acad Sci USA* 96:11820–11824.

Youssef et al.

www.manaraa.com